Received: 21 February 2018 | Accepted: 24 May 2018

DOI: 10.1111/desc.12703

PAPER

WILEY Developmental Science

Development of brain functional connectivity and its relation to infant sustained attention in the first year of life

Wanze Xie[1,2,3] | Brittany M. Mallin[4] | John E. Richards[1,2]

[1]Department of Psychology, University of South Carolina, Columbia, South Carolina

[2]Institute for Mind and Brain, University of South Carolina, Columbia, South Carolina

[3]Boston Children's Hospital, Harvard Medical School, Boston, Massachusetts

[4]Ultrasound Leadership Academy, Salt Lake City, Utah

Correspondence
Wanze Xie, Boston Children's Hospital, Harvard Medical School, 1 Autumn Street, 6th Floor, Boston, MA 02215, USA.
Email: wanze.xie@childrens.harvard.edu or xiew@mailbox.sc.edu

Funding information
This work was supported by NIH grant, #R37 HD18942.

Abstract

The study of brain functional connectivity is crucial to understanding the neural mechanisms underlying the improved behavioral performance and amplified ERP responses observed during infant sustained attention. Previous investigations on the development of functional brain connectivity during infancy are primarily confined to the use of functional and structural MRI techniques. The current study examined the relation between infant sustained attention and brain functional connectivity and their development during infancy with high-density EEG recordings. Fifty-nine infants were tested at 6 (*N* = 15), 8 (*N* =14), 10 (*N* = 17), and 12 (*N* = 13) months. Infant sustained attention was defined by measuring infant heart rate changes during infants' looking. Functional connectivity was estimated from the electrodes on the scalp and with reconstructed cortical source activities in brain regions. It was found that infant sustained attention was accompanied by attenuated functional connectivity in the dorsal attention and default mode networks in the alpha band. Graph theory analyses showed that there was an increase in path length and a decrease in clustering coefficient during infant sustained attention. The functional connectivity within the visual, somatosensory, dorsal attention, and ventral attention networks and graph theory measures of path length and clustering coefficient were found to increase with age. These findings suggest that infant sustained attention is accompanied by distinct patterns of brain functional connectivity. The current findings also suggest the rapid development of functional connectivity in brain networks during infancy.

1 | INTRODUCTION

Infant sustained attention is a type of endogenous attention that is characterized by a deceleration in heart rate (HR) and represents the arousal state of infants (Colombo, 2001). There is empirical evidence showing the important role that infant sustained attention plays in information processing and attention allocation (Xie & Richards, 2016a), as well as its effects on infants' high-level cognitive processes, such as memory encoding and learning (Richards, 1997). A recent study by Xie, Mallin, and Richards (2018) sheds light on the neural mechanisms underlying infant sustained attention by showing its relation to electroencephalography (EEG) oscillatory activity in the theta and alpha rhythms. The existing literature suggests that the effects of infant sustained attention may result from or be associated with distinct pattern(s) of functional connectivity in brain networks. The application of network analysis provides an illuminating perspective on the dynamic interregional communications or connectivity inside the brain. The current study aimed to test the potential connection between infant sustained attention and brain functional connectivity and how it may develop in the first year of life. Brain functional connectivity was estimated on the sensor level and in the source space using MRI-constrained cortical source reconstructions. Graph theory measures were applied to obtain a view of the architecture of brain functional networks.

1.1 | Definition of infant sustained attention and its behavioral and neural correlates

Infant sustained attention has been predominantly studied using the measure of HR derived from electrocardiogram (ECG) recordings (Reynolds & Richards, 2008). Infant attention state can be categorized into sustained attention and inattention based on HR changes during infants' looking towards visual presentations (Guy, Zieber, & Richards, 2016; Xie & Richards, 2016a). Infant sustained attention is the phase when infant HR decelerates significantly and remains at a lower level compared to the prestimulus baseline. The phase of inattention is when infant HR accelerates to the prestimulus level and the period before HR deceleration starts.

Infant sustained attention is accompanied by improved performances of infants in behavioral tasks. The majority of infants' information processing takes place during sustained attention (Colombo, 2001). Infants were observed to be more engaged in stimulus presentation (Xie & Richards, 2016a) and less likely to be distracted by a peripheral distracting stimulus during sustained attention than inattention (Pérez-Edgar et al., 2010). Infants also demonstrated better memory for the events they were exposed to during sustained attention (Reynolds & Richards, 2005; Richards, 1997).

The neural correlates of infant sustained attention have been studied with EEG and event-related potential (ERP) measures. The negative central (Nc) component was found to be larger in amplitude during sustained attention than inattention (Richards, 2003). The Nc effect might reflect the attention-getting properties of the stimulus and the activation of a general arousal system or the alerting system in the brain (Reynolds & Romano, 2016; Richards, 2003). Infant sustained attention also has been found to amplify the amplitude of infant face-sensitive components, the N290 and P400 (Guy et al., 2016), and the P1 and N1 components that reflect the early visual processing of a stimulus (Xie & Richards, 2016b). A recent study linked the EEG oscillations in the theta and alpha bands to sustained attention performance in infants (Xie et al., 2018). Increased theta power and attenuated alpha power were found during sustained attention in infants aged 10 and 12 months. The attenuated alpha power during sustained attention was localized to the brain regions composing the default mode network (DMN) using cortical source analysis. These ERP and EEG findings support the idea that infant sustained attention is accompanied by an increase of brain tonic alertness and information processing efficiency (Richards, 2008).

These behavioral and physiological effects suggest that the signal transmission or functional connectivity in the brain might be different during infant sustained attention than inattention. However, there is no empirical evidence for the connection between functional brain connectivity and infant sustained attention. A study looking at the functional brain connectivity during infant sustained attention would advance our understanding of the neural mechanisms of sustained attention from a brain network perspective.

RESEARCH HIGHLIGHTS

- Infant sustained attention was accompanied by a decrease of functional brain connectivity within the dorsal attention and default mode networks in the alpha band.
- Path length increased and clustering coefficient decreased during sustained attention on the sensor level and in the source space.
- The functional connectivity within the somatomotor, dorsal attention, and ventral attention networks in the alpha band increased with age from 6 to 12 months.
- There was a decrease in path length and an increase in clustering coefficient from 6 to 12 months.
- This study demonstrates the possibility of studying functional connectivity within brain networks in oscillatory frequency bands in infants using EEG cortical source analysis.

1.2 | The study of brain functional networks in pediatric populations

The application of resting-state fMRI to study functional brain connectivity has advanced our understanding of the dynamic interregional communications inside the brain and their development during infancy. A study by Fransson and colleagues (2007) reported distinct resting-state networks primarily located in the somatosensory regions with no evidence of the presence of the DMN in infants younger than 12 months. This finding suggests that the primary sensory and sensorimotor systems are already functionally delineated during early infancy while the high-level functional networks (e.g. the DMN) undergo a much-delayed development. Convergent evidence for the development of brain functional networks during infancy has been provided by more recent studies (e.g. Damaraju et al., 2014; Gao, Alcauter, Smith, Gilmore, & Lin, 2015). Graph theory provides a common framework to examine the efficiency of the dynamic processes in a network and characterize the overall architecture of the network (Bullmore & Sporns, 2009). The analysis of resting-state fMRI signals with graph theory measures has found a decrease of randomness and an increase of order over the first 2 years of life (Cao et al., 2017; Gao et al., 2011).

The construction of brain functional networks can also be achieved with electrophysiological recordings (e.g. EEG and MEG; Hillebrand, Barnes, Bosboom, Berendse, & Stam, 2012) which provide direct measurements of neuronal activity with exceptional temporal resolution. A recent study investigated the development of functional connectivity in the somatosensory cortex during early infancy (younger than 12 months) and young childhood (24–34 and 36–60 months) with MEG (Berchicci, Tamburro, & Comani, 2015). The authors reported that the functional connectivity in the somatosensory network remains almost unchanged during infancy

but undergoes dramatic changes in the segregation and integration properties of the network from 1 year to 2 years of age. The measurement of MEG functional connectivity, along with graph theory measures, has also been applied to characterize alterations in brain networks in children with reading difficulties (Dimitriadis et al., 2013) and autism spectrum disorder (Ye, Leung, Schafer, Taylor, & Doesburg, 2014). One potential limitation of using MEG to study functional connectivity with young children comes from the fact that spurious connections could be caused by head movements (Messaritaki et al., 2017).

High-density EEG recordings offer a comparatively easy-to-use alternative to measure brain functional networks with greater tolerance to young children's movements. Analyses of the EEG recordings with graph theory measures have found changes in path length and clustering coefficient over childhood (Boersma et al., 2011; Miskovic et al., 2015; Smit et al., 2012). For example, Boersma and colleagues (2011) found that the mean clustering coefficient in the alpha band and path length in the theta, alpha and beta bands were found to increase from 5 to 7 years of age. Progress has recently been made by conducting cortical source analysis with age-specific children MRI templates so that brain networks can be constructed based on connectivity between neural substrates (Bathelt, O'Reilly, Clayden, Cross, & de Haan, 2013). Bathelt et al. (2013) reported an increase of the node degree and clustering coefficient and a decrease of path length from 2 to 6 years of age, which were comparable to the fMRI literature on the network development at this age (Power, Fair, Schlaggar, & Petersen, 2010).

The recent advances made in the study of the development of functional brain connectivity have shed light on the rapid changes occurring in brain networks from early infancy to adolescence (see Vertes & Bullmore, 2015, for a review). To the best of our knowledge, the development of functional connectivity in brain networks during infancy has not been studied with EEG recordings. Therefore, it is still unclear whether the development of brain functional connectivity during infancy measured with EEG recordings would converge on the previous fMRI reports with infants and EEG findings with children.

The studies reviewed above suggest that the development of functional connectivity may be influenced by infant sustained attention. Several of these studies imply there may be increased connectivity between the major components of the DMN during infancy (Fransson et al., 2007; Gao et al. 2011). There also may be development in networks primarily defined in adult connectivity studies. One popular network atlas was created by Yeo and colleagues with resting-state fMRI signals (Yeo et al., 2011). They identified five networks based on their distinguished pattern of intrinsic functional connectivity: visual, somatosensory, dorsal attention, ventral attention, and DMN. For example, the visual network consists of regions in the striate and extrastriate cortices, and the somatosensory network includes regions along the pre- and post-central gyri. Infants' visual perception and behavioral control are improved during sustained attention (Richards, 2008). It is likely that the connectivity within the visual and somatomotor networks (Yeo et al., 2011) would become functionally established during early infancy, evident by 6 months of age, and affected by sustained attention. Infant sustained attention facilitates the allocation of spatial attention and enhances the ERPs' amplitudes elicited in a spatial cueing paradigm among infants younger than 6 months of age (Mallin & Richards, 2012; Xie & Richards, 2016b). Therefore, infant sustained attention may also show an impact on the connectivity in the dorsal and ventral attention networks from 6 months of age. Alternatively, the effect of sustained attention on the connections in the DMN may not be found until 10 to 12 months due to its more protracted development (Gao et al., 2011; Xie et al., 2018). The current study will be the first to examine the existence of these networks in infants and their possible relation to the development of sustained attention.

1.3 | Current study

The objective of this current study was to directly link infant sustained attention to functional brain connectivity. Infant sustained attention and the phase of inattention were defined based on infant HR changes during infants' looking at stimulus presentation (Reynolds & Richards, 2008). The connectivity was examined in the infant theta, alpha, and beta frequency bands using both the sensor activities and the cortical source activities in different brain regions. Cortical source reconstruction was conducted with realistic head models created with age-appropriate average MRI templates (Richards, Sanchez, Phillips-Meek, & Xie, 2016). Seed-based functional connectivity analysis was conducted for the visual, somatomotor, dorsal attention, ventral attention, and DM networks. Graph theory measures of path length, clustering coefficient, and small-worldness were used to estimate the overall topology of brain functional networks. Functional connectivity during infant sustained attention was hypothesized to be attenuated in the alpha band and increased in the theta band. This hypothesis was made based on previous studies showing opposite effects of attention on the activities in the two frequency bands (Orekhova, Strognova, & Posikera, 1999, 2001; Xie et al., 2018). The network integration and segregation estimated by graph theory measures were also hypothesized to be different between infant sustained attention and inattention.

The EEG data were collected in a cross-sectional way at four ages (6, 8, 10, and 12 months) to investigate the development of brain functional connectivity during infancy. These ages were chosen to cover a critical period for the development of infant sustained attention (Colombo, 2001). This is also an important age for the development of infant EEG power in different frequency bands (Marshall, Bar-Haim, & Fox, 2002). The effect of infant sustained attention on EEG power is predominantly found at 10 and 12 but not 6 and 8 months of age (Xie et al., 2018). Therefore, it is an open question whether the relation between infant sustained attention and functional connectivity would also differ with age. It was hypothesized that the attention effect on connectivity would be primarily found for the two older age groups for the DMN but might be shown in the other networks at younger ages. Another hypothesis was that functional connectivity in the five brain networks would increase from 6 to 12 months of age based on the previous evidence for the development of brain functional connectivity over childhood.

2 | METHODS

2.1 | Participants

The final sample had 59 participants and contained the following numbers of participants for each age group: 6 (N = 15, M = 184.4 days, SD = 15.51), 8 (N = 17, M = 239.4, SD = 15.02), 10 (N = 14, M = 289.3, SD = 14.53), and 12 (N = 13, M = 350.6, SD = 13.77) months. An additional eight participants were tested but they became fussy before the end of the data collection. Two participants did not finish the experiment due to equipment failure (e.g. programs crashed). Another nine participants were excluded from analyses due to excessive artifacts (e.g. eye or body movements and noise) in their data. Thus, 69 participants were tested in total ranging in age from 6 to 12 months. These data also were analyzed in Xie et al. (2018) for different research objectives.

2.2 | Apparatus and stimuli

A color monitor, two cameras, and computers were used for stimulus presentation and video recording. Microsoft Visual C ++ programs were used for presentation and experimental control. The stimuli included seven *Sesame Street* dancing and singing sequences made from the movie, *Sesame Street's 25th Anniversary* over a static background (Courage, Reynolds, & Richards, 2006). The character in a scene might talk (or sing) at one location, disappear from the scene, move from one location to another on the screen, or disappear as it was moving across the screen.

2.3 | Procedure

One randomly selected *Sesame Street* movie sequence was presented at the beginning of each experimental block. When the infant looked toward this movie, a randomly selected *Sesame Street* character was presented on the left or the right side of the monitor. The character stayed at that location singing or dancing for 8–12 s. The character then moved to the other side of the monitor and stayed there for 8–12 s. The character moved back to the original side for an additional 8–12 s. The character might also disappear, that is, hide behind the scene for a few seconds. The data collected during the disappearance of the character were excluded from further analyses. One experimental block lasted for 2 minutes with multiple characters. New *Sesame Street* movies and character sequences were presented in the next experimental block. This sequence of presentations was repeated until the participant got fussy. The whole experiment lasted for about 10–15 min.

2.4 | Judgment of visual fixation

Participants' looking was judged based on the review of the video recordings. Data were only used for further analyses when a participant looked toward the presentation.

2.5 | ECG recording and HR defined attention phases

The ECG data were recorded with two Ag-AgCL electrodes placed on each infant's chest. The R-R interval is the latency period between the R waves of two heartbeats, and it was used to compute the inter-beat interval (IBI). The lengthening and shortening of the IBI correspond to the HR deceleration and acceleration, respectively. Attention phases were defined based on HR (IBI) changes during infants' looking. The phase of sustained attention was defined as the time when there was a significant deceleration of HR compared to the prestimulus level and the HR remaining at the lowered level. The phase of inattention consisted of the phase of pre-attention (automatic interrupt and stimulus orienting) and attention termination (Reynolds & Richards, 2008).

2.6 | EEG recording and preprocessing

The EEG was recorded simultaneously with the ECG. The Electrical Geodesics Incorporated (EGI, Eugene, OR) EEG system was used for EEG recording. The data were recorded with the 128-channel 'Geodesic Sensor Net (GSN)' for 34 participants and with the 128-channel 'HydroCel Geodesic Sensor Net (HGSN)' for 25 participants. The EEG was measured from 124 channels in the electrode net. The other four channels were left for the Ag-AgCl electrodes used to measure ECG and electrooculogram (EOG). The EEG was recorded with 20 K amplification at a 250 Hz sampling rate with band-pass filters set from 0.1 to 100 Hz. The channel impedance was measured and accepted if it was below 100 kΩ. The EEG recording was referenced to the vertex and then algebraically recomputed to an average reference.

The EEG recordings were preprocessed using the EEGLAB toolbox (Delorme & Makeig, 2004) in MATLAB (R2015b, the Mathworks, Inc.). The continuous EEG data were filtered with band-pass filters set from 1 to 50 Hz. The filtered data were then segmented into 1s epochs (Bathelt et al., 2013). The EEG epochs were inspected for artifacts (ΔEEG > 200 μV or ΔEEG > 100 μV within 50 ms). Independent component analysis (ICA) was conducted using the 'runica' program in MATLAB to remove components of eye movements (Xie et al., 2018). Channel interpolation was conducted using the five closest channels if there were fewer than 12 channels that were missing or had bad data. Each attention phase must have at least 10 clean trials for the data to be included for further analyses (DeBoer, Scott, & Nelson, 2007).

2.7 | Cortical source reconstruction

Figure 1 demonstrates the pipeline for source-space functional connectivity analysis. It illustrates the procedures and the outputs for the methods described in the following sections including cortical source reconstruction, parcellation of cortical reconstructions into brain ROIs, and functional connectivity analysis.

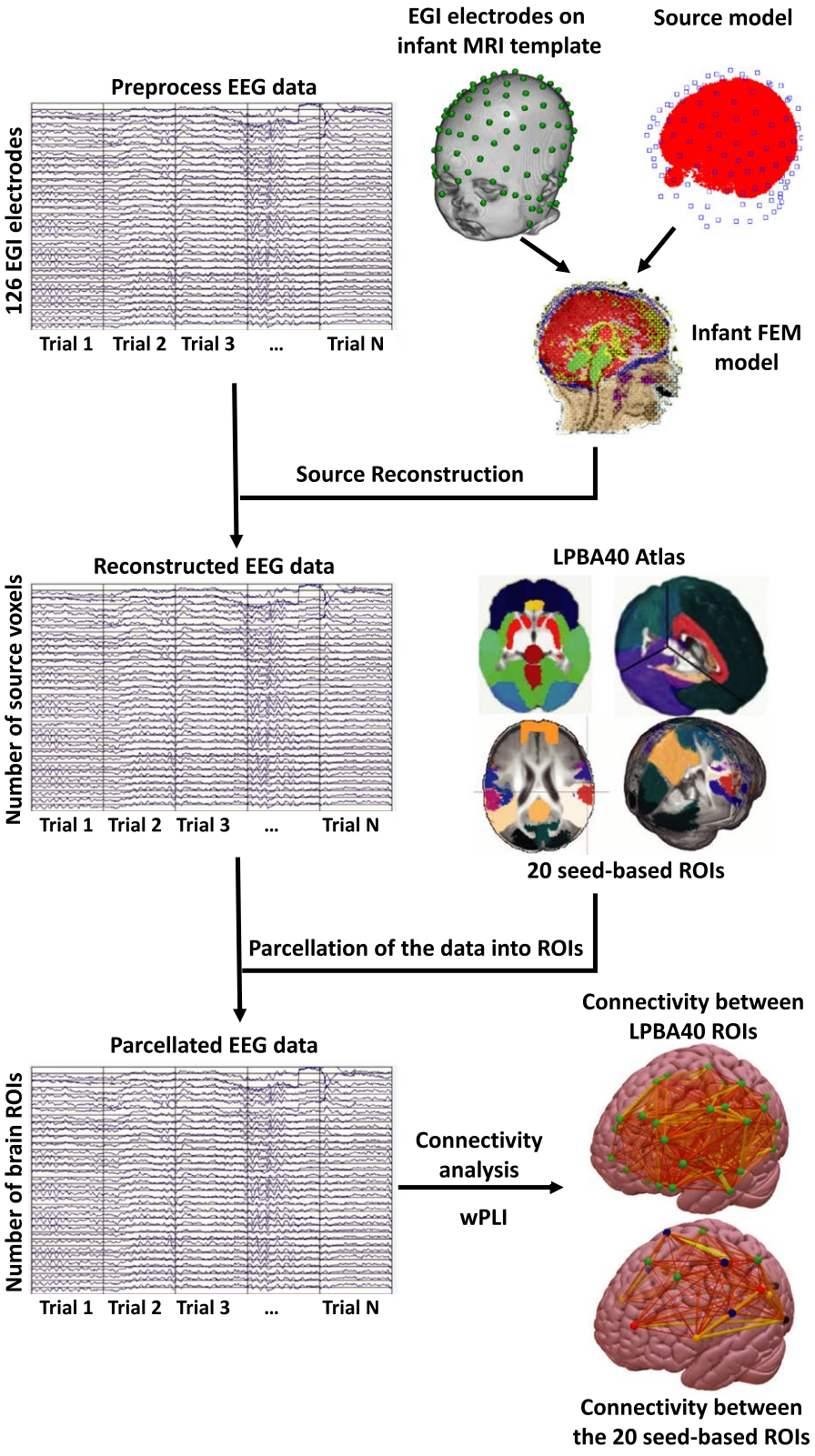

FIGURE 1 Pipeline for the functional connectivity analysis in the source space

The cortical source reconstruction of EEG recordings for different frequency bands was conducted with the Fieldtrip (Oostenveld, Fries, Maris, & Schoffelen, 2011) toolbox. The steps of source analysis included the selection of anatomical MRI, construction of realistic head models, distributed source reconstruction, and segmenting source activity of the whole brain into ROIs. Details about each step have been described by Xie and Richards (2016b). These steps were also compatible with those employed by Bathelt et al. (2013) and Hillebrand et al. (2012) with older children and young adults.

An age-related average MRI template was selected for each age group from the Neurodevelopmental MRI Database (Richards et al., 2016; Richards & Xie, 2015). These MRI templates were used to create the realistic head models. Anatomical MRIs were segmented into component materials with the GM and eyes being used as source volumes. A forward model was created for each MRI template with a Finite Element Method (FEM) model, source volumes with 5 mm spatial resolution, and an electrode placement map (Richards, Boswell, Stevens, & Vendemia, 2015). The forward model was then used to estimate the lead field matrix and the spatial filter matrix (inverse of the lead field matrix).

Cortical source reconstruction was conducted using the current density reconstruction (CDR) technique with the head models, lead field matrix, and the spatial filter matrix. Distributed source reconstruction of the EEG time-series in each epoch was conducted with the exact-LORETA (eLORETA; Pascual-Marqui, et al., 2011) as the constraint. This process resulted in source activities in three moments (directions) for each source voxel. The dimension that explains the most variance of the source activities in a voxel was used to represent its activation (Bathelt et al., 2013).

2.8 | Parcellation of cortical source activity into ROIs

The reconstructed cortical time-series in GM voxels were parcellated into brain ROIs. Anatomical brain MRIs were segmented into ROIs using the LPBA brain atlas (Shattuck et al., 2008). This resulted in 48 cortical ROIs. The reconstructed time-series in the source voxels were averaged for each brain ROI (Bathelt et al., 2013; Dai et al., 2017). The reconstructed time-series also were parcellated into 20 cortical areas that are the major components of five brain networks defined by Yeo and colleagues (2011). The five networks included the visual, somatomotor, dorsal attention, ventral attention, and the DMN networks. The Yeo networks (Yeo et al., 2011), Automatic Anatomical Labeling (AAL; Tzourio-Mazoyer et al., 2002), LPBA (Shattuck et al., 2008), and the Hammers (Hammers et al., 2003) atlases were used to define the 20 cortical ROIs (i.e. components) included in these networks. The ROIs for the five brain networks are illustrated in Figure 2. The ROIs and the atlases used to construct the ROIs are described in Supplemental Table 2.

2.9 | Functional connectivity analysis

Functional connectivity analysis was conducted separately for the infant theta (2–6 Hz), alpha (6–9 Hz), and beta (9–13 Hz) bands using the Fieldtrip toolbox. The functional connectivity was estimated with the weighted phase lag index (wPLI; Vinck, Oostenveld, van Wingerden, Battaglia, & Pennartz, 2011) between the 126 EEG electrodes, the 20 ROIs for the five brain networks, as well as the 48 cortical ROIs defined by the LPBA atlas. Given that infant theta (Xie et al., 2018) and alpha (Marshall et al., 2002) band power dominates the frequency band spectrum, the wPLI measure was applied to reduce the effects of volume conduction and absolute EEG amplitude (power) on the estimation of functional connectivity between EEG signals. The wPLI measure weighs the phase differences according to the magnitude of the leads and lags so that phase differences around zero generated by noise perturbations in the signals would only have a marginal contribution to the wPLI results (Vinck et al., 2011). The calculation of connectivity resulted in N × N weighted adjacency matrices where N stands for the number of electrodes or brain ROIs. Each value or element in these adjacency matrices represented the wPLI value between a pair of electrodes or brain ROIs. The Fisher's *r*-to-*z* transformation was applied to these 'correlation' values in the adjacency matrices to improve the normality of their distribution. The adjacency matrices for the functional connectivity between the EEG electrodes were reorganized into 13 virtual electrode clusters (e.g. left frontal, right frontal, and occipital-inion). The GSN and HGSN electrodes included in these clusters and their corresponding 10–10 positions are listed in Supplemental Table 1. A range of sparsity thresholds (0.1 ≤ threshold ≤ 0.4, step = 0.05) was applied to the adjacency matrices to take the noise and spurious connectivity into account (Rubinov & Sporns, 2010). More detailed information about the procedures for the functional connectivity analysis are described in the Supplemental Information.

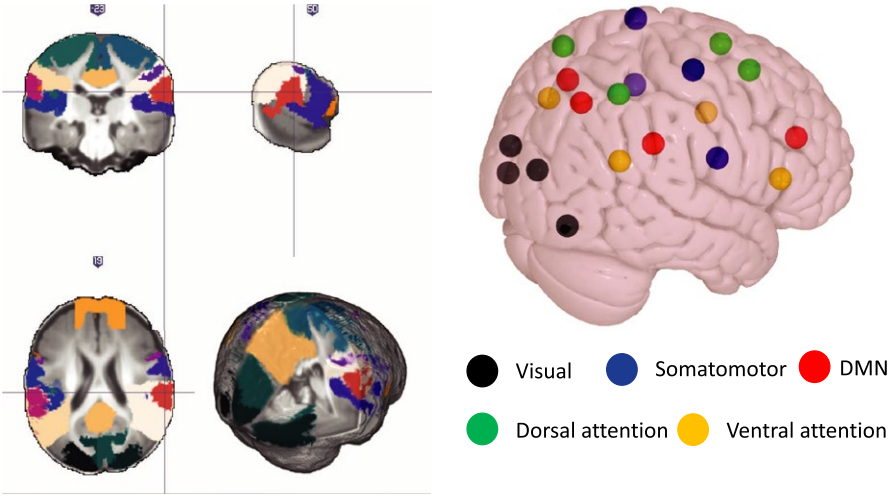

FIGURE 2 The 20 ROIs included in the five brain networks displayed in an infant brain MRI and a 3D brain surface image

2.10 | Seed-based functional connectivity analysis

Seed-based functional connectivity analysis was conducted in the source space. The wPLI value between each pair of the 20 ROIs was extracted from the adjacency matrices. This allowed us to compare the connectivity between certain pairs of ROIs and to compare the averaged connectivity within a network (e.g. the DMN) between different conditions (e.g. sustained attention vs. inattention).

Seed-based functional connectivity analysis also was conducted on the sensor level. The wPLI value between the 126 electrodes (seeds) was extracted from the adjacency matrices and grouped into the 10 virtual clusters. The wPLI value between the electrodes in a virtual cluster was calculated.

2.11 | Graph theory measurements

The brain network topology was estimated with graph theory measures. Graph theory measurements of the properties (e.g. path length, clustering coefficient) of functional networks were applied with the Brain Connectivity Toolbox (BCT; Rubinov & Sporns, 2010) and the GRETNA toolbox (Wang et al., 2015) in MATLAB (R2016a, the Mathworks, Inc.).

Graph theory measurements were examined in the source space and on the channel level. The nodes of a network were defined as the 126 electrodes or the 48 LPBA cortical ROIs. The edges were defined as the functional connections (wPLI values) between all pairs of the nodes. The clustering coefficient for a node was calculated as the proportion of its neighboring nodes that were connected to each other. The averaged clustering coefficient (Cp) that reflects the average level of local organization of a network was then calculated. The shortest path length between two nodes was calculated as the lowest value among the sums of different path lengths between them. The averaged shortest path length (Lp) of the entire network was then calculated to reflect the average level of global organization of the network. A normalization process of the Lp and Cp was conducted to calculate the small-worldness (sigma) with 200 randomized networks being generated with the same number of nodes and distribution of edges as the real functional networks (Maslov & Sneppen, 2002; Sporns & Zwi, 2004). The small-worldness of a network represents the balance between high local organization (segregation) and global organization (integration) for a network (Stam et al., 2009). A sigma value greater than 1 indicates a network having the property of small-worldness (Watts & Strogatz, 1998). The area under the curve (AUC) was calculated for these graph theory measures, which provided a summarized scalar for the graph theory measures regardless of the network intensity (Zhang et al., 2011). The major steps for the data analysis in the current study are summarized in Figure 3.

2.12 | Design for statistical analysis

Statistical analysis was performed with mixed-design ANOVAs using the Proc GLM function in SAS (SAS institute Inc, Cary, NC). The averaged wPLI value within a network was analyzed as the dependent variable in the seed-based connectivity analyses for the five brain networks. Post-hoc tests (e.g. multiple comparisons) for the wPLI value between individual pairs of ROIs were conducted with false discovery control (FDR, $p < 0.05$). The AUC values for the path length (Lp), clustering coefficient (Cp), and small-worldness (sigma) were analyzed as the dependent variables in the graph theory analyses. The seed-based connectivity and graph theory analyses both included attention phase (2: attention and inattention) and frequency band (3: theta, alpha, and beta) as within-subject independent variables, and age (4: 6, 8, 10 and 12 months) as a between-subjects independent variable. All significant tests were reported at $p < 0.05$.

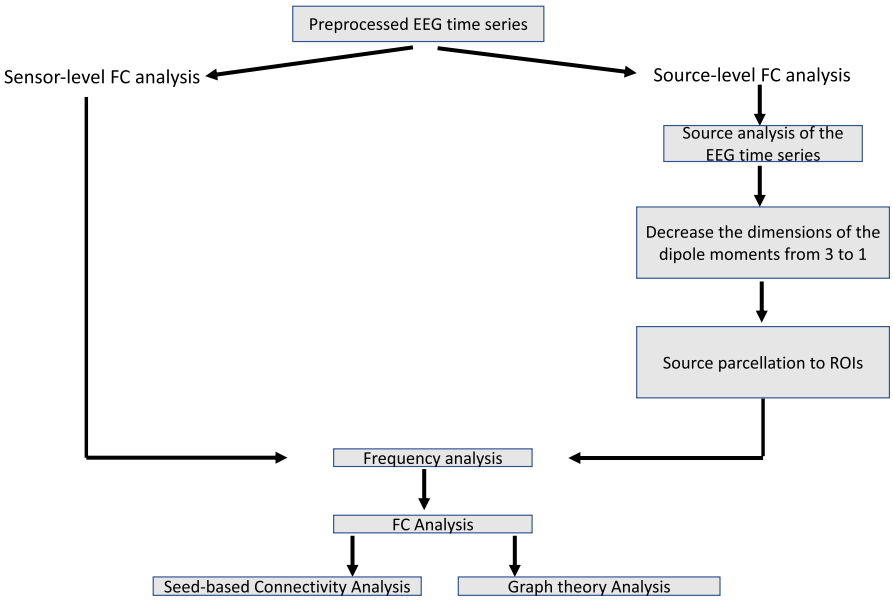

FIGURE 3 Summary of the pipelines for the data analysis in the current study

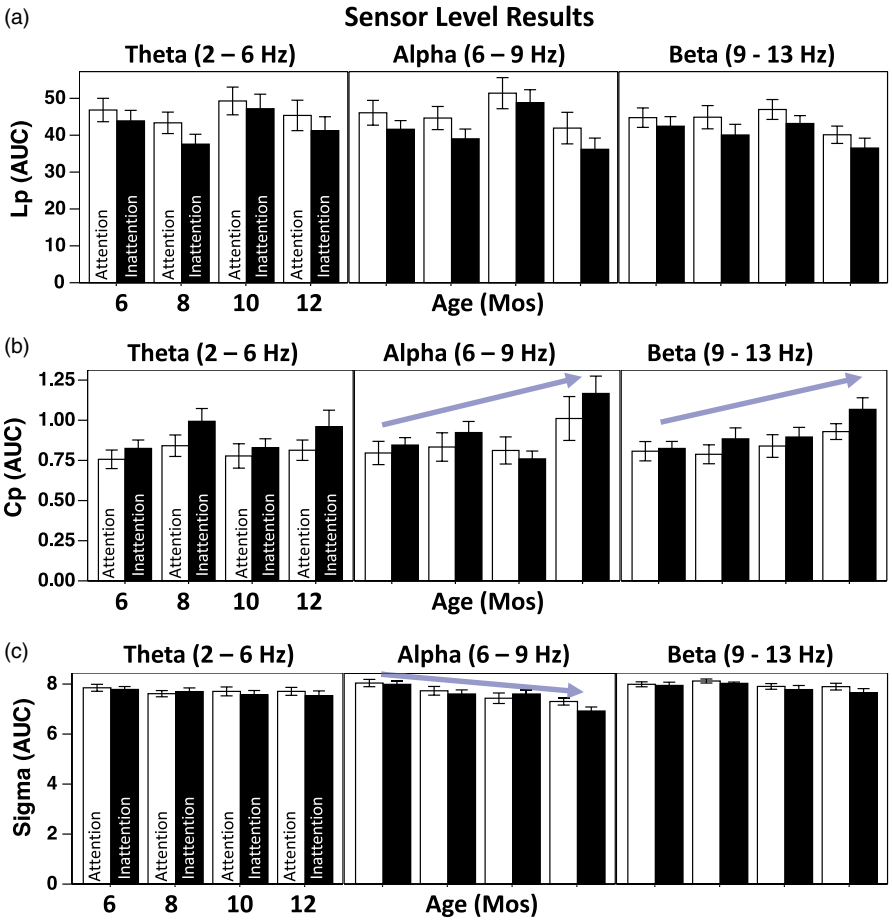

FIGURE 4 The changes of the path length (Lp), clustering coefficient (Cp), and small-worldness (sigma) on the sensor level as a function of attention phase, and age, and frequency band. The Individual bars are for the AUC value of the Lp (a), Cp (b), and sigma (c) across conditions, respectively. The blue arrow lines indicate the age effect

3 | RESULTS

Sufficient numbers of trials were obtained for the conditions of sustained attention and inattention. The number of trials obtained for sustained attention (M = 174.49, 95% CI [140.15 196.26]) was not significantly different than that for inattention (M = 151.78, 95% CI [117.39 186.17]).

3.1 | Graph theory analysis

3.1.1 | Sensor-level analysis

Path length (Lp) on sensor level

An analysis was conducted to determine the effect of attention and age on the global network efficiency in different frequency bands. The AUC value for Lp was analyzed as a function of attention phase, age, and frequency band with a mixed-design ANOVA. The analysis for the Lp showed a main effect of attention phase, $F(1, 55)$ = 7.95, p = 0.0067, partial η^2 = 0.13. The AUC value for Lp was greater during sustained attention than inattention (Figure 4a, also see Supplemental Information for changes of Lp across network intensities). There was no age or interaction between the three factors.

Clustering coefficient (Cp) on sensor level

The analysis for the Cp showed a main effect of attention phase, $F(1, 55)$ = 7.29, p = 0.0092, partial η^2 = 0.117. The AUC value for Cp was greater during inattention than sustained attention. The interaction between age and frequency band was close to being significant, $F(6, 110)$ = 2.16, p = 0.0525, partial η^2 = 0.105. Follow-up analyses showed that the age effect was significant for the alpha, $F(6, 110)$ = 9.79, p = 0.0010 and beta, $F(6, 110)$ = 6.43, p = 0.0144, bands. The AUC value for Cp was greater for the 12 months compared to the other three ages for the alpha and beta bands. Figure 4b shows that the Cp value increased with age in the alpha and beta bands, and it was greater during inattention than sustained attention (also see Supplemental Information for changes of Cp as a function of network intensity).

Small-worldness (sigma) on sensor level

The analysis for the sigma value showed a significant interaction between age and frequency band, $F(6, 110)$ = 2.58, p = 0.0223, partial η^2 = 0.123. A simple effect test showed that the AUC value for sigma decreased with age only for the alpha band, $F(3, 110)$ = 11.27, p < 0.00010 (Figure 4c). Figure 5a depicts the changes in the sigma value as a function of network intensity from 10% to 100%, separately for the attention phases, ages, and frequency bands. It shows that when the network intensity was low (e.g. 10%, 15%, and 20%) the sigma value was greater than 1, a sign of showing small-worldness, at 6 and 8 months in the alpha and beta bands.

3.1.2 | Source space analysis

Path length (Lp) in source space

The analysis on the AUC value for Lp in the source space revealed a main effect of attention phase, $F(1, 55) = 8.96$, $p = 0.0041$, partial $\eta^2 = 0.14$. The AUC value for Lp was greater for sustained attention than inattention (Figure 6a, also see Supplemental Information for the changes of Lp across network intensities). There was also an interaction between age and frequency band, $F(6, 110) = 3.39$, $p = 0.0042$, partial $\eta^2 = 0.16$. A simple effect test showed that the AUC value for Lp significantly decreased with age for the alpha, $F(3, 110) = 6.10$, $p = 0.00070$, and theta, $(3, 110) = 7.45$, $p = 0.00010$, bands (Figure 6a).

Clustering coefficient (Cp) in source space

The analysis on the AUC value for Cp revealed an interaction between attention phase and frequency band, $F(2, 110) = 3.83$, $p = 0.025$, partial $\eta^2 = 0.065$. This interaction was driven by the greater AUC value for Cp during inattention than sustained attention for the alpha, $F(1, 110) = 28.78$, $p < 0.0001$, but not for the theta and beta bands (Figure 6b). There was also an interaction between age and frequency band, $F(6, 110) = 4.61$, $p = 0.00030$, partial $\eta^2 = 0.20$. A simple effect test showed that the AUC value for Cp increased with age for theta, $F(3, 110) = 6.43$, $p = 0.00050$, and alpha, $F(3, 110) = 5.68$, $p = 0.0012$, bands (Figure 6b).

Small-worldness (sigma) in source space

The analysis on the AUC value for sigma did not show a main effect of attention phase or age, or an interaction between them. Figure 6c shows that there was no clear change in the AUC value for sigma with age or any difference between the two attention phases. Figure 5b depicts the changes in the sigma value as a function of network intensity from 10% to 100%. The sigma value overall appears to be not different from 1, but when the network intensity was low (e.g. 10%, 15%, and 20%) it is greater than 1 at 6 months in the alpha (for inattention) and beta bands.

3.2 | Connectivity analysis

The connectivity analysis was conducted for the 20 ROIs (seeds) in five brain networks and the electrodes on the scalp, with emphasis on the ROIs within the brain networks. The averaged functional connectivity within a brain network was analyzed as a function of attention phase, age, and frequency band. When a significant effect of attention was found for a network post-hoc multiple comparisons between sustained attention and inattention were conducted for individual pairs of connections in a network with FDR control. The results for the connectivity analysis on the sensor level were briefly reported because the primary goal of the seed-based connectivity analysis was to examine the functional connectivity in brain networks.

3.3 | Seed-based connectivity analysis for brain networks in the source space

3.3.1 | Visual network

The mean wPLI value for the connections within the visual network was analyzed to determine whether there were differences

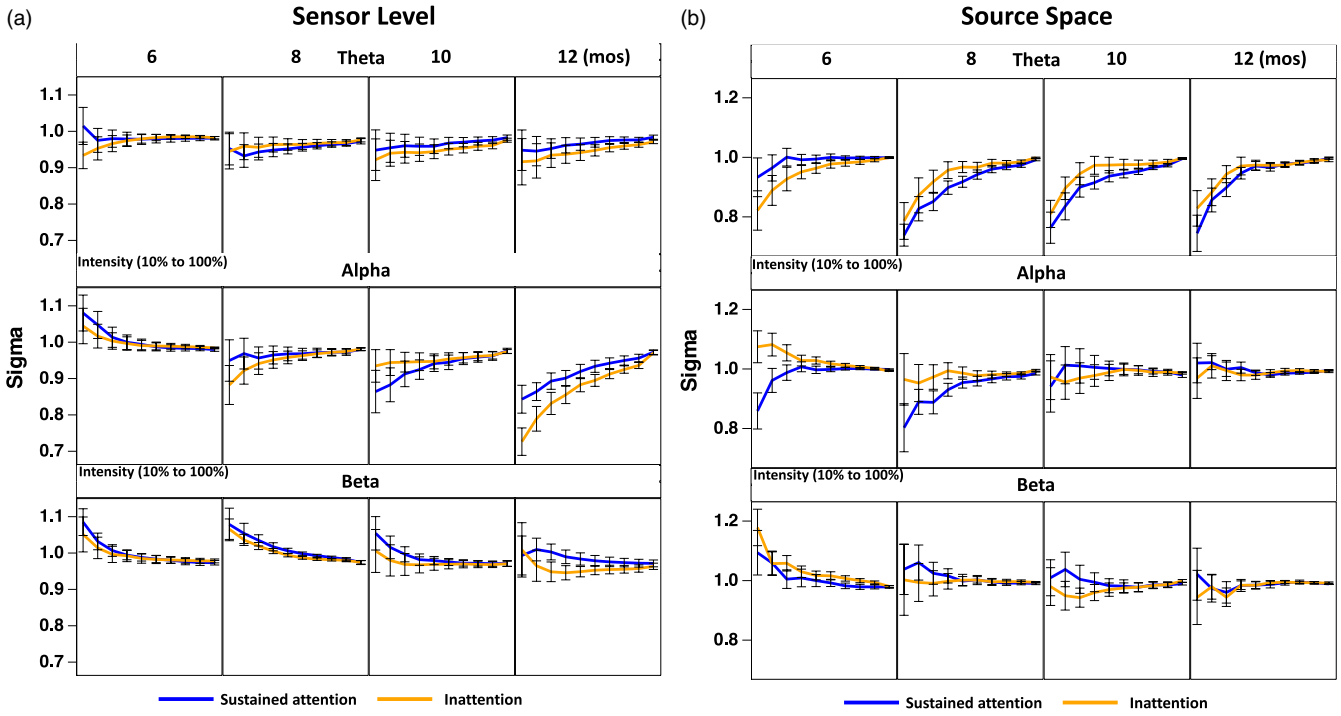

FIGURE 5 The changes of the small-worldness (sigma) as a function of network intensity from 10% to 100%. This information is shown separately for the results on the sensor level (a) and those in the source space (b). The blue lines refer to the results for sustained attention, while the orange lines refer to the results for inattention

between attention phases and ages in different frequency bands. The mean wPLI value was analyzed as a function of attention phase, age, and frequency band with a mixed-design ANOVA. This analysis revealed a significant interaction between age, attention phase, and frequency band, $F(6, 110) = 2.72$, $p = 0.017$, partial $\eta^2 = 0.129$. Subsequent analyses showed that the interaction between age and attention phase was not significant for the alpha band, $F(3, 55) = 2.75$, $p = 0.051$. A simple effect test showed that the mean wPLI value increased with age only during inattention, $F(3, 55) = 2.91$, $p = 0.042$. Figure 7a depicts individual bars that represent the mean wPLI value within the visual network for different attention phases, ages and frequency bands. The mean wPLI value was greater for 12 months than the other ages during inattention in the alpha band (Figure 7a).

3.3.2 | Somatomotor network

This analysis on the mean wPLI value within the somatomotor network showed a significant interaction between age and frequency band, $F(6, 110) = 2.28$, $p = 0.041$, partial $\eta^2 = 0.108$. A simple effect test showed that the age effect was significant only for the alpha band, $F(3, 55) = 4.88$, $p = 0.0032$. The mean wPLI value increased with age. Figure 7b shows that the mean wPLI value network increases with age in the alpha band.

3.3.3 | Dorsal attention network

The analysis for the dorsal attention network showed that the attention effect on functional connections varied across the three frequency bands. There was a significant interaction between attention phase and frequency band, $F(2, 110) = 5.78$, $p = 0.0041$, partial $\eta^2 = 0.096$. Subsequent analyses showed that the mean wPLI value was greater during inattention than sustained attention for the alpha band only (Figure 7c). Post-hoc comparisons ($p < 0.05$, corrected by FDR) were conducted to analyze the attention effect for individual pairs of connections between the ROIs within the dorsal attention network in the alpha band. It was found that the wPLI value between the left SPG/IPS and left FEF was significantly greater during inattention than sustained attention (Figure 8a). Figure 8b depicts the difference in the wPLI value between sustained attention and inattention (inattention − sustained attention) for the connections within the dorsal attention network and the DMN in a 3D brain surface. It can be seen that the greater connectivity in the alpha band is clearly shown between the left FEF and the left SPG/IPS.

The ANOVA for the dorsal attention network also revealed an interaction between age and frequency band, $F(6, 110) = 4.34$, $p = 0.00060$, partial $\eta^2 = 0.194$. This interaction was driven by an age effect found in the alpha band only, $F(3, 55) = 11.73$, $p < 0.0001$. The

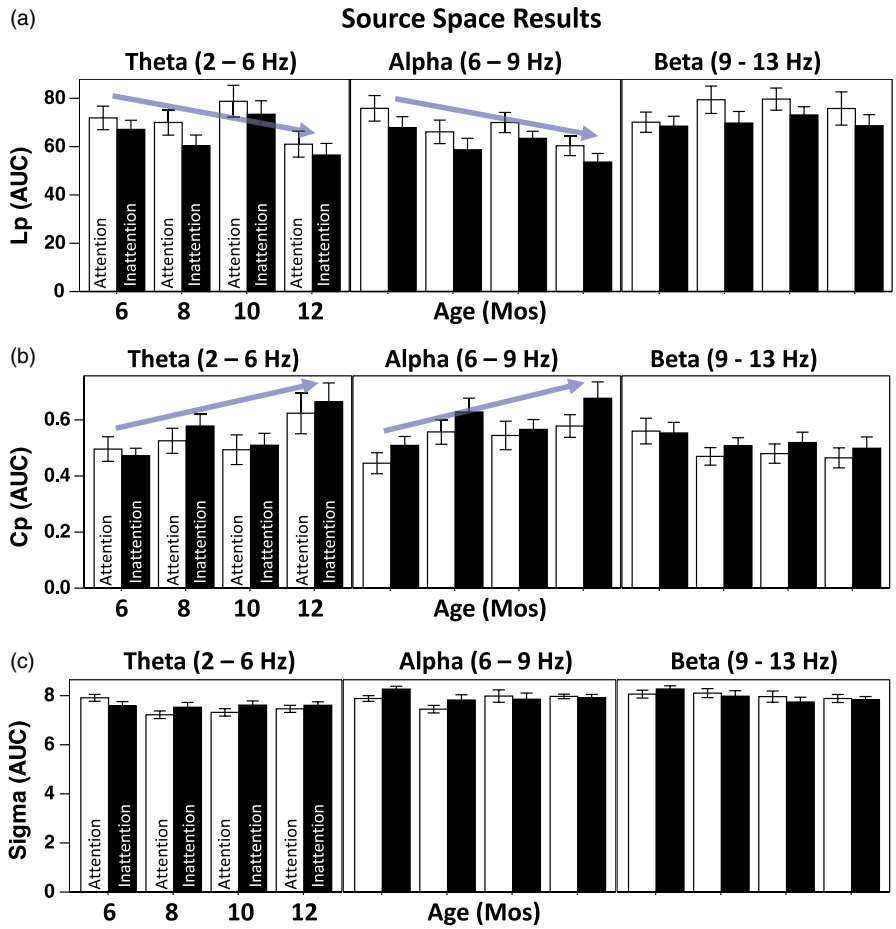

FIGURE 6 The changes of the path length (Lp), clustering coefficient (Cp), and small-worldness (sigma) in the source space as a function of attention phase, and age, and frequency band. The Individual bars are for the AUC value of the Lp (a), Cp (b), and sigma (c) across conditions, respectively. The blue arrow lines indicate the age effect

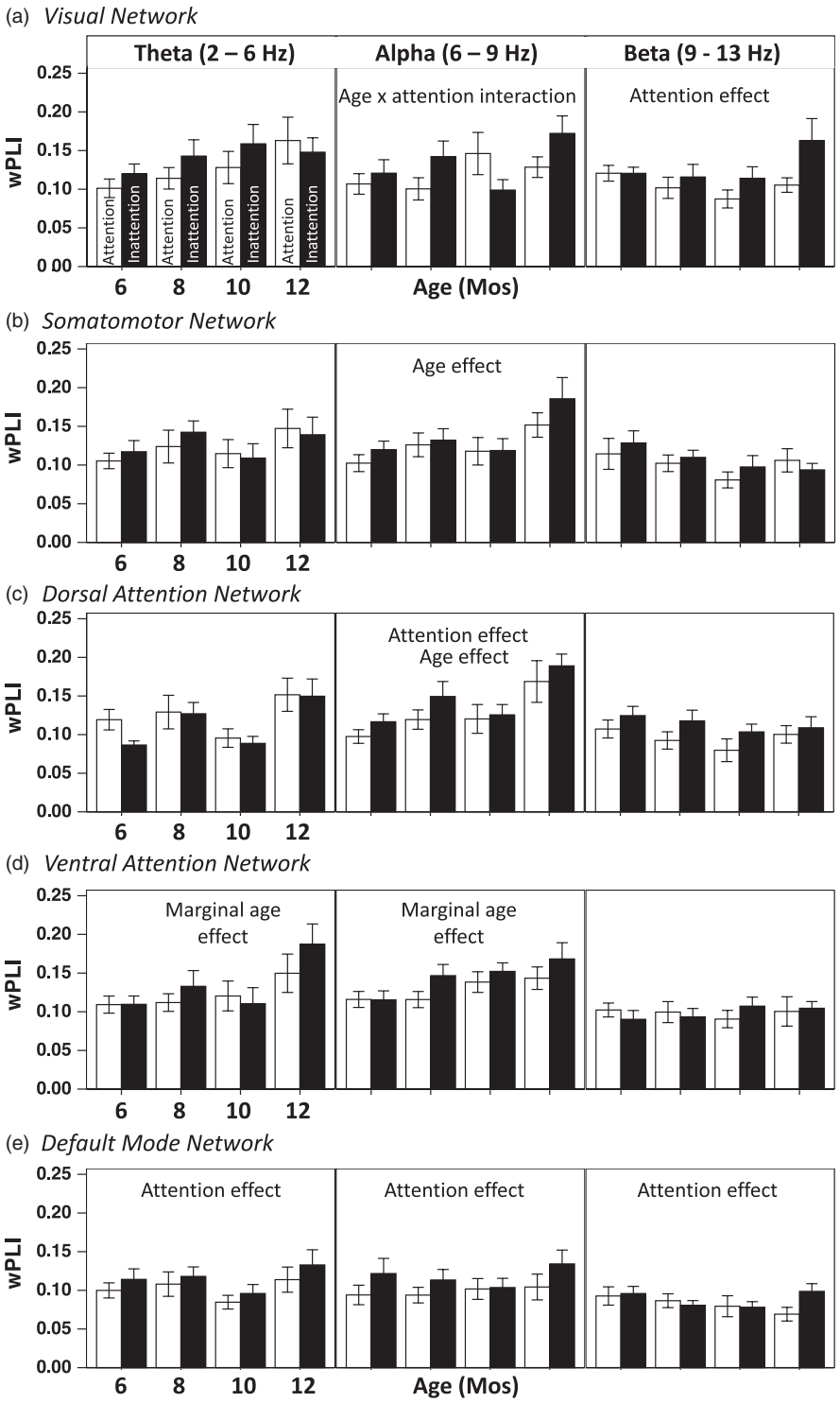

FIGURE 7 Individual bars that represent the mean connectivity (wPLI value) within the five brain networks for different attention phases, ages, and frequency bands

mean wPLI value was found to increase with age for the alpha band (Figure 7c).

3.3.4 | Ventral attention network

The analysis for the ventral attention network did not show a significant effect for attention phase, $F(1, 55) = 3.84$, $p = 0.055$, or age $F(3, 55) = 2.48$, $p = 0.070$. The mean wPLI value appears to increase with age in the theta and alpha bands, although it did not reach the significance level (Figure 7d).

3.3.5 | Default model network

The analysis for the DMN showed a significant main effect for attention phase, $F(1, 55) = 6.08$, $p = 0.0168$, partial $\eta^2 = 0.10$. The mean wPLI value was greater during inattention than sustained attention.

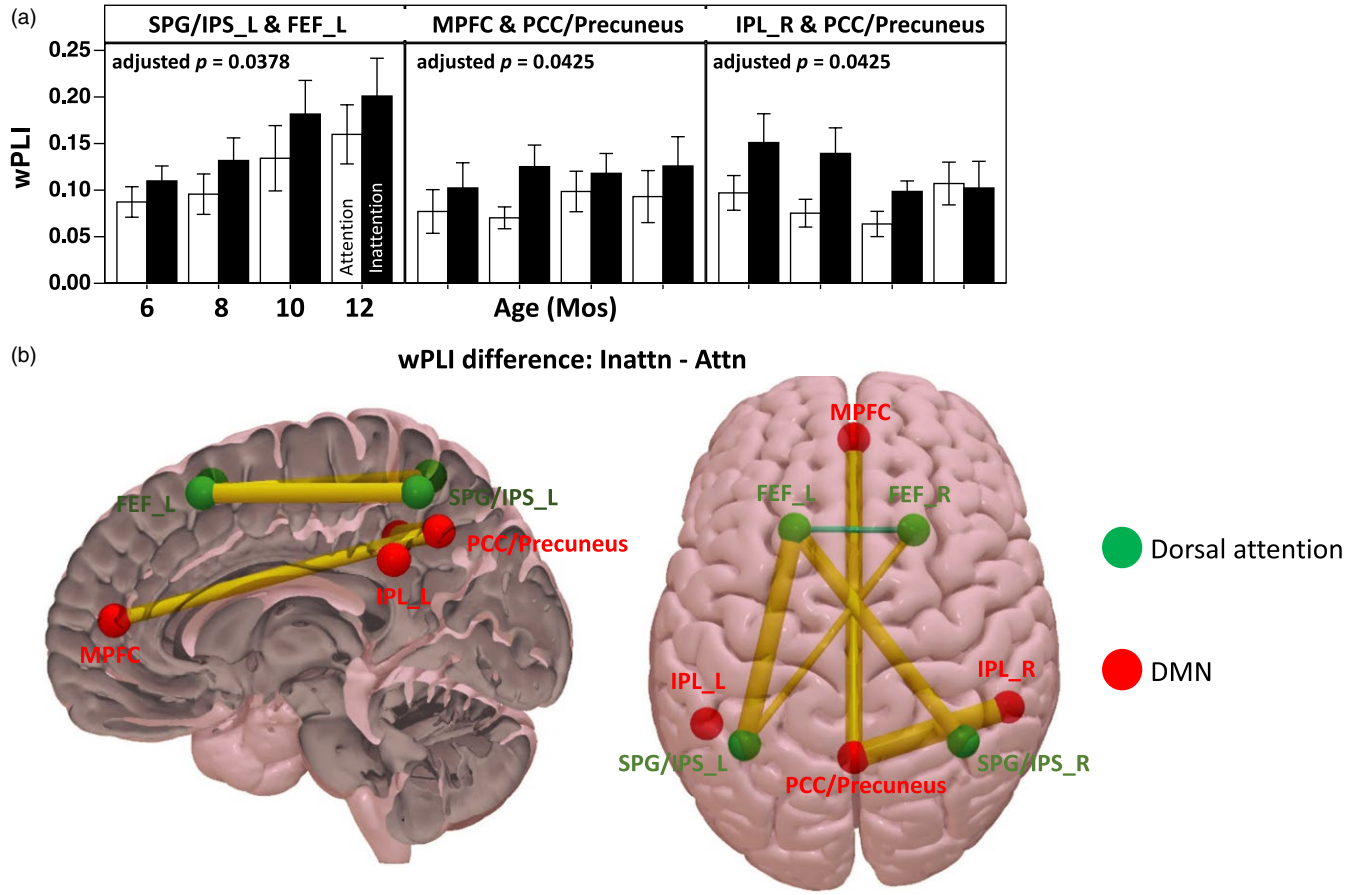

FIGURE 8 Functional connectivity in the alpha band for the dorsal attention and default mode networks. (a) The wPLI value for the three pairs of connections that showed significant difference between sustained attention and inattention in the alpha band. (b) The difference in the wPLI value between sustained attention and inattention in the alpha band. The spheres represent the nodes (ROIs) within the dorsal attention network (green) and the DMN (red). The lines represent the difference in the wPLI value between sustained attention and inattention (inattention − sustained attention) for the connections between the nodes. The thickness of the lines represents the value of the difference, with thicker lines represent greater values. *Note*: These connections showed a p value less 0.05 for the attention effect, but only the difference between the three pairs of connections shown in (A) reached the significance level after FDR control (adjusted $p < 0.05$)

This attention effect was not found to interact with frequency band (Figure 7e). Post-hoc comparisons ($p < 0.05$, corrected by FDR) were conducted to analyze the attention effect for individual pairs of connections between the ROIs within the DMN. It was found that the wPLI values in the alpha band between the medial prefrontal cortex and the PCC/Precuneus and between the right inferior parietal lobule and the PCC/Precuneus were significantly greater during inattention than sustained attention (Figure 8a). The comparisons for the connections in the theta and beta bands did not show any significant result after the FDR control. The difference between attention and inattention in these connections also are depicted in a 3D brain surface in Figure 8b.

3.3.6 | Connections between the 20 ROIs

The difference between sustained attention and inattention also appeared to exist in the functional connectivity between the five brain networks. Figure 9 shows the difference in the wPLI value between sustained attention and inattention for all 20 ROIs with a network intensity of 10% for the alpha band. Both circular maps (top panel) and adjacency matrices demonstrate that about half of the connections greater for inattention involve the ROIs in the DMN, especially the PCC/Precuneus. No statistical analysis was conducted for these connections between networks. The results for the theta and beta bands are described in the Supplemental Information.

3.3.7 | Summary of the seed-based connectivity analysis for the brain networks

Functional connectivity between brain ROIs were found to change with age and attention phase. Infant sustained attention was found to have an impact on the averaged functional connectivity within the DMN and the dorsal attention network in the alpha band. In addition, the averaged functional connectivity in the alpha band within the visual, somatosensory, dorsal attention, and ventral attention networks was found to increase with age.

3.4 | Connectivity analysis for the virtual channel clusters on the sensor level

The analyses for the connections between the electrodes in the 13 virtual clusters did not reveal an age effect for any of the frequency bands. The attention effect was analyzed with the FDR control for these clusters and frequency bands. Only the connectivity in the alpha band within the left Parietal ($F(1, 55) = 9.09$, adjusted $p = 0.0370$) and left central ($F(1, 55) = 4.61$, adjusted $p = 0.0385$) virtual clusters showed a significant difference between sustained attention and inattention. Figure 10 depicts the reorganized adjacency matrices for the difference in the alpha band connectivity between inattention and sustained attention (top panel). It shows that the alpha band connectivity during sustained attention was attenuated in the central and parietal (left and central) clusters. The differences in the alpha band connectivity between sustained attention and inattention predominantly involve the left and central (Z) parietal and central clusters, that is, the lines go from other clusters to left and central (Z) parietal and central clusters (Figure 10).

4 | DISCUSSION

The present study investigated the relation between infant sustained attention and infant brain functional connectivity and its development in the second half of the first postnatal year. The primary goal was to investigate the functional connectivity during infant sustained attention. Distinct patterns of brain network topology were found with graph theory measures for sustained attention. The path length was longer and the clustering coefficient was lower during sustained attention rather than inattention. Seed-based connectivity analysis showed that the connectivity within the DMN and the dorsal attention network was attenuated in the alpha band during sustained attention than inattention. The connectivity between networks also appeared to be weaker during sustained attention in the alpha band. In contrast to our hypothesis, there was no interaction of sustained attention and age. Main effects of age were found on functional connectivity in the alpha band within the visual, somatosensory, and dorsal attention networks from 6 to 12 months. The path length was found to decrease with age and the clustering coefficient was found to increase with age in the theta and alpha bands. Infants at 6 and 8 months showed the feature of small-worldness in their brain networks with low network intensity. The major results have been summarized in Table 1.

4.1 | Functional connectivity in major brain networks during infant sustained attention

The finding of the attenuated functional connectivity in the alpha band during sustained attention in the DMN indicates the important role that the DMN plays in infant attention. Attenuated alpha power during infant sustained attention has been shown by previous EEG research (Xie et al., 2018), although increased alpha power during infants' internally driven attention was reported by another study (Orekhova et al., 2001). The attenuated alpha activity was localized to the brain regions composing the DMN using the technique of EEG

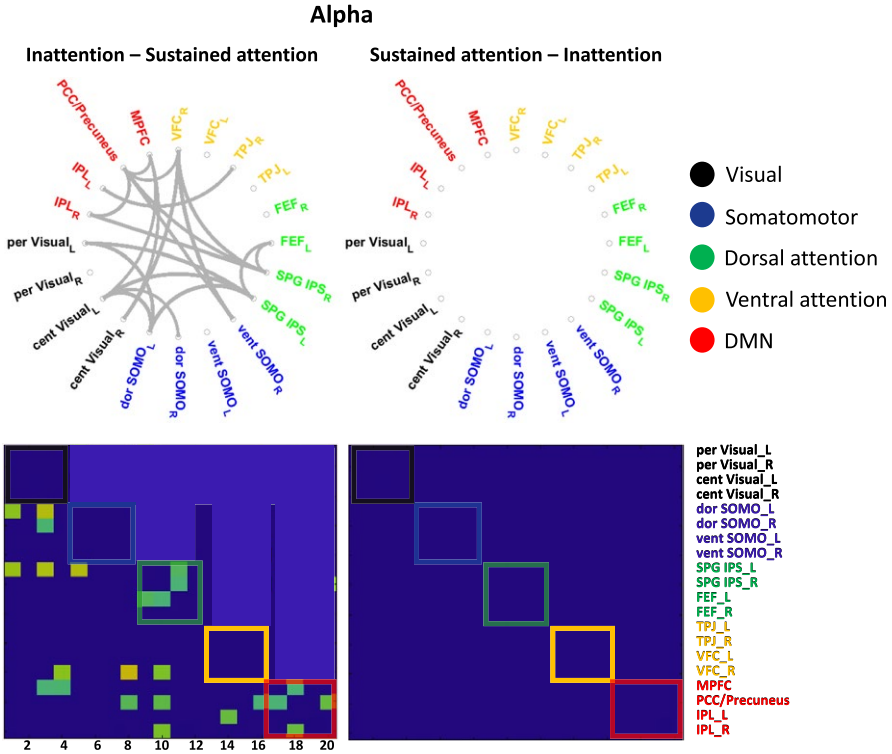

FIGURE 9 The difference in the wPLI value between sustained attention and inattention for all 20 ROIs with a network intensity of 10% for the alpha band

source analysis (Xie et al., 2018). The finding in the current study suggests that the functional connectivity in the alpha band between the components of the DMN also is attenuated during sustained attention (Figure 8). This finding supports the idea that enhanced brain alertness and attention allocation during infant sustained attention might be caused by attenuated activity in the DMN.

Infant sustained attention is also associated with a decrease of functional connectivity in the alpha band in the dorsal attention network. The current study uses a paradigm including dancing *Sesame Street* characters presented in different locations. The areas included in the dorsal attention network (e.g. the FEF and SPG/IPS) are crucial for spatial attention orienting, goal-directed selection for stimuli, and planning for eye movements (Corbetta & Shulman, 2002). Therefore, this network is very likely to be active during the presentation in this experiment, although the trials with eye movements have been excluded from the analyses. The finding of the decreased connectivity in the alpha band might suggest the releasing of the dorsal attention system (i.e. task-relevant areas) from inhibition (Klimesch, Sauseng, & Hanslmayr, 2007).

The weakened connectivity in the alpha band found for the frontal, central, and parietal sensor clusters might be associated with the decreased connectivity in the DMN and the dorsal attention network. The connectivity between the electrodes in the frontal and temporal areas and those in the central and parietal areas appeared to be weakened for the alpha band during infant sustained attention (Figure 10). This finding suggests that the changes occurred in underlying neural mechanisms during infant sustained attention. The cortical source analysis conducted in the current study provides a link between the finding on the scalp and the changes in the brain. The attenuated frontoparietal connectivity between the components in the DMN (the MPFC and PCC/Precuneus) and the dorsal attention network (the FEF and the SPG/IPS) might cause the distinct patterns observed on the sensor level.

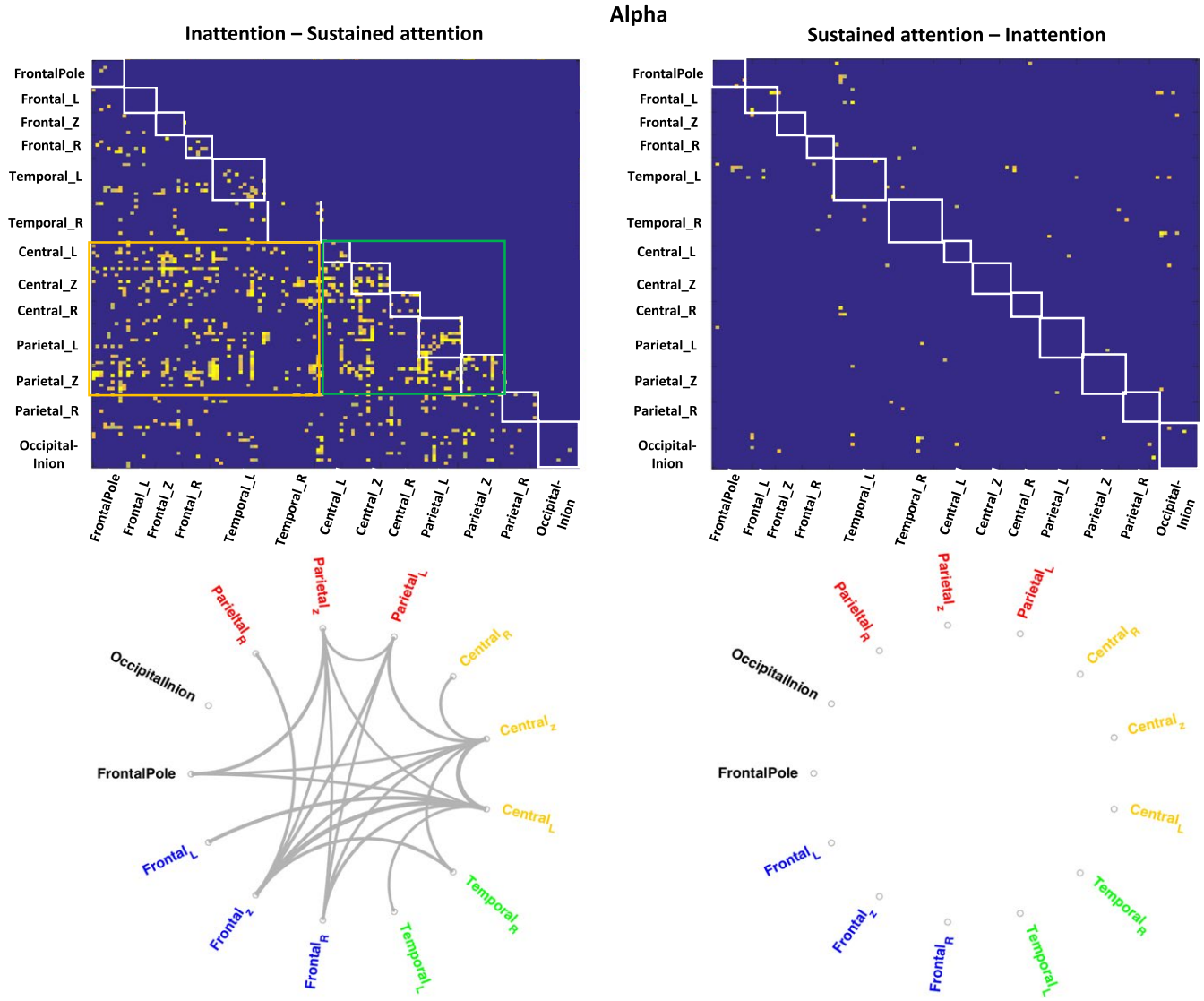

FIGURE 10 The difference in the wPLI value between sustained attention and inattention for the 13 virtual clusters made of the 126 electrodes, with a network intensity of 10% for the alpha band

TABLE 1 Summary of the major findings from the graph theory and seed-based connectivity analyses

Analyses	Measures/Networks	Results	Figures
Graph theory (sensory level)	Path Length (Lp)	(i) Lp was greater during sustained attention than inattention.	Figure 4a
	Clustering Coefficient (Cp)	(i) Cp was smaller during sustained attention than inattention.	Figure 4b
		(ii) Cp was greater for 12 mos than other ages in the alpha and beta bands.	Figure 4b
	Small-worldness (sigma)	(i) Sigma value was greater than 1 for 6 and 8 mos for the alpha and beta bands.	Figure 4c
Graph theory (source space)	Path Length (Lp)	(i) Lp was greater during sustained attention than inattention.	Figure 6a
		(ii) Lp decreased with age in the alpha and theta bands.	
	Clustering Coefficient (Cp)	(i) Cp was smaller during sustained attention than inattention for the alpha band.	Figure 6b
		(ii) Cp increased with age in the alpha and theta bands.	
	Small-worldness (sigma)	(i) Sigma value was greater than 1 for 6 mos in the alpha and beta bands.	Figure 6c
Seed-based connectivity analysis	Visual	(i) Connectivity increased with age during inattention in the alpha band.	Figure 7a
	Somatomotor	(i) Connectivity increased with age during inattention in the alpha band.	Figure 7b
	Dorsal Attention	(i) Connectivity was greater during inattention than sustained attention in the alpha band.	Figure 7c
		(ii) Connectivity increased with age in the alpha band.	
	Ventral Attention	(i) Marginal effect on attention and age.	Figure 7d
	Default Mode	(i) Connectivity was greater during inattention than sustained attention in the alpha band.	Figure 7e, Figure 8

4.2 | Distinct network topology during infant sustained attention

Infant sustained attention is accompanied by a declined brain network integration and segregation. The finding of shorter path length and higher clustering coefficient during inattention than sustained attention suggests that the long-distance (integration) and local (segregation) communications between cortical regions are weakened during sustained attention. This finding is inconsistent with our hypothesis that was made based on the improved information processing found during sustained attention by previous research (e.g. Richards, 2008; Xie & Richards, 2016a). One explanation of this finding is that infant brain networks become more randomized with higher cost for local and global communications during inattention. This type of network organization has been found in children with attention deficit hyperactivity disorder (ADHD). Decreased path length and increased clustering coefficient have been found in ADHD children using EEG measures (Ahmadlou, Adeli, & Adeli, 2012), The atypical network topology found in these studies with ADHD children has been a reflection of a more randomized network organization with higher cost for connections.

The current study suggests novel neural correlates of infant sustained attention with respect to graph theory measures. Infant sustained attention has been associated with amplified ERP responses (Guy et al., 2016) and attenuated alpha power (Xie et al., 2018). The current study suggests that infant sustained attention is also associated with longer path length and lower clustering coefficient. These features of network topology might indicate a less randomized and overall more cost-effective organization of brain networks during sustained attention. Infant sustained inattention is characterized by a deceleration of HR caused by an increase of the function of the parasympathetic system (Richards, 2008). The changes in the neurotransmitter system should have an impact on the communication between subcortical (e.g. the thalamus) and cortical regions. This in turn might result in the distinct patterns of brain network topology found during infant sustained attention.

4.3 | The functional connectivity in major brain networks increases with age

The current study suggests a rapid change in the strength of functional connectivity within the major brain networks during the first year of age. An increase of the strength of functional connectivity was found in the alpha band for the visual, somatosensory, dorsal attention, and ventral attention networks. The remarkable development of functional connections in these major brain networks is consistent with past fMRI research on infants (Damaraju et al., 2014; Fransson et al., 2007). The DMN did not show an increase of functional connectivity within the network. The absence of the age effect for the DMN is in line with previous fMRI research showing that the functional connectivity in the DMN is not exhibited until 12 months of age (Gao et al., 2011). The development of brain functional connectivity in these networks varies across the frequency bands. The absence of an age effect on the beta band connectivity is compatible with the idea that the functional significance of the beta band oscillations is still unclear during infancy (Cuevas, Cannon, Yoo, & Fox, 2014).

A cross-sectional strategy was used to collect data at the four different ages. This is a potential limitation of the current study given

the fact that a longitudinal design would be more powerful to the show the changes in functional connectivity over time. Future research should be conducted to look at the development of connectivity during infancy with longitudinally collected EEG data.

4.4 | Development of brain network topology in the second half of the first year

There is an increase of functional integration and segregation of information processing over development from 6 to 12 months of life from a graph theory perspective. The finding of a decrease of path length and an increase of clustering coefficient in the theta and alpha bands indicates the changes in the global and local efficiency of signal transmission in brain networks. This finding is consistent with the increase of brain network segregation and integration during infancy shown by resting-state fMRI research (Gao et al., 2011). The small-world connectional architecture for brain networks was observed in the current study in the alpha and beta bands at 6 and 8 months with low network intensities. This finding is consistent with previous fMRI studies showing an early presence of the small-worldness for brain networks in newborn (Fransson, Aden, Blennow, & Lagercrantz, 2011) and preterm infants (Cao et al., 2017; van den Heuvel et al., 2015). However, the absence of the small-worldness at 10 and 12 months is inconsistent with the fMRI literature that has suggested a continued development of the small-worldness throughout the first few years of life (Fair et al., 2009; Power et al., 2010). This discrepancy suggests that differences in characteristics of brain networks might be found between using EEG and fMRI measures.

The current findings extend our understanding of the development of functional networks in different frequency rhythms during infancy. The changes of network organization found in the current study are parallel to the existing EEG literature on the development of functional connectivity from early childhood (e.g. 2 to 4 years) to adolescence (Bathelt et al., 2013; Boersma et al., 2011; Miskovic et al., 2015; Smit et al., 2012). It should be noted that there were also inconsistent findings among these EEG studies. For example, some studies have found an increase of path length in the alpha band over childhood and adolescence (Boersma et al., 2011; Smit et al., 2012), while the current study and others have shown a decrease of path length in the alpha band with age (Bathelt et al., 2013; Miskovic et al., 2015). The different techniques (e.g. Pearson correlation, imaginary part of the coherency, wPLI, and synchronization likelihood) used to measure the functional connectivity between EEG signals might have contributed to these inconsistent findings (Bastos & Schoffelen, 2016; Vinck et al., 2011).

5 | CONCLUSION

The current study advances our understanding of the function of infant sustained attention by establishing the first connection between infant sustained attention and brain functional connectivity. The attenuated within network connectivity in the alpha band was observed primarily in two attention-related networks, the dorsal attention network and the DMN. The attention effect on the overall network topology in a graph theory perspective was found from 6 months of age.

The current study also suggests that cortical source analysis with EEG data can be used with infant participants to study the functional connectivity in brain networks. Functional networks can be constructed on the sensor level and in the source space (see the Supplemental Information for more discussion). The method used in the current study suggests an alternative way to examine the development of brain networks. This method should be particularly useful for infant studies because of the easy application of EEG and its tolerance to movement compared to fMRI with infants. Similar findings on the development of brain networks have been shown by the current study in comparison to previous infant MRI research. These findings might serve as a reference that allows us to identify the disruptions in the brain networks of children with neurodevelopmental disorders (e.g. Autism Spectrum Disorder and ADHD).

ACKNOWLEDGEMENTS

This work was supported by the NIH grant, #R37 HD18942, to JER.

CONFLICTS OF INTEREST

The authors have approved the manuscript and agreed with its submission. These authors declare no conflict of interest.

ORCID

Wanze Xie http://orcid.org/0000-0002-9983-7948

REFERENCES

Ahmadlou, M., Adeli, H., & Adeli, A. (2012). Graph theoretical analysis of organization of functional brain networks in ADHD. *Clinical EEG and Neuroscience*, *43*(1), 5–13.

Bastos, A.M., & Schoffelen, J.M. (2016). A tutorial review of functional connectivity analysis methods and their interpretational pitfalls. *Frontiers in Systems Neuroscience*, *9*, 175.

Bathelt, J., O'Reilly, H., Clayden, J.D., Cross, J.H., & de Haan, M. (2013). Functional brain network organisation of children between 2 and 5 years derived from reconstructed activity of cortical sources of high-density EEG recordings. *NeuroImage*, *82*, 595–604.

Berchicci, M., Tamburro, G., & Comani, S. (2015). The intrahemispheric functional properties of the developing sensorimotor cortex are influenced by maturation. *Frontiers in Human Neuroscience*, *9*, 39.

Boersma, M., Smit, D.J., de Bie, H.M., Van Baal, G.C., Boomsma, D.I., de Geus, E.J., & Stam, C.J. (2011). Network analysis of resting state EEG in the developing young brain: Structure comes with maturation. *Human Brain Mapping*, *32*(3), 413–425.

Bullmore, E., & Sporns, O. (2009). Complex brain networks: Graph theoretical analysis of structural and functional systems. *Nature Reviews Neuroscience*, *10*(3), 186–198.

Cao, M., He, Y., Dai, Z.J., Liao, X.H., Jeon, T.N., Ouyang, M.H., & Huang, H. (2017). Early development of functional network segregation revealed by connectomic analysis of the preterm human brain. *Cerebral Cortex*, *27*(3), 1949–1963.

Colombo, J. (2001). The development of visual attention in infancy. *Annual Review of Psychology*, *52*, 337–367.

Corbetta, M., & Shulman, G.L. (2002). Control of goal-directed and stimulus-driven attention in the brain. *Nature Reviews Neuroscience*, *3*(3), 201–215.

Courage, M.L., Reynolds, G.D., & Richards, J.E. (2006). Infants' attention to patterned stimuli: Developmental change from 3 to 12 months of age. *Child Development*, *77*(3), 680–695.

Cuevas, K., Cannon, E.N., Yoo, K., & Fox, N.A. (2014). The infant EEG mu rhythm: Methodological considerations and best practices. *Developmental Review*, *34*(1), 26–43.

Dai, Z.X., de Souza, J., Lim, J.L., Ho, P.M., Chen, Y., Li, J.H., & Sun, Y. (2017). EEG Cortical Connectivity Analysis of Working Memory Reveals Topological Reorganization in theta and alpha bands. *Frontiers in Human Neuroscience*, *11*, 237.

Damaraju, E., Caprihan, A., Lowe, J.R., Allen, E.A., Calhoun, V.D., & Phillips, J.P. (2014). Functional connectivity in the developing brain: A longitudinal study from 4 to 9 months of age. *NeuroImage*, *84*, 169–180.

Deboer, T., Scott, L.S., & Nelson, C.A. (2007). Methods for acquiring and analysing infant event-related potentials. In M. De Haan (Ed.), *Infant EEG and event-related potentials* (pp. 5–37). London: Psychology Press.

Delorme, A., & Makeig, S. (2004). EEGLAB: An open source toolbox for analysis of single-trial EEG dynamics including independent component analysis. *Journal of Neuroscience Methods*, *134*(1), 9–21.

Dimitriadis, S.I., Laskaris, N.A., Simos, P.G., Micheloyannis, S., Fletcher, J.M., Rezaie, R., & Papanicolaou, A.C. (2013). Altered temporal correlations in resting-state connectivity fluctuations in children with reading difficulties detected via MEG. *NeuroImage*, *83*, 307–317.

Fair, D.A., Cohen, A.L., Power, J.D., Dosenbach, N.U.F., Church, J.A., Miezin, F.M., & Petersen, S.E. (2009). Functional brain networks develop from a 'local to distributed' organization. *Plos Computational Biology*, *5*(5), e1000381.

Fransson, P., Aden, U., Blennow, M., & Lagercrantz, H. (2011). The functional architecture of the infant brain as revealed by resting-state fMRI. *Cerebral Cortex*, *21*(1), 145–154.

Fransson, P., Skiold, B., Horsch, S., Nordell, A., Blennow, M., Lagercrantz, H., & Aden, U. (2007). Resting-state networks in the infant brain. *Proceedings of the National Academy of Sciences, USA*, *104*(39), 15531–15536.

Gao, W., Alcauter, S., Smith, J.K., Gilmore, J.H., & Lin, W. (2015). Development of human brain cortical network architecture during infancy. *Brain Structure and Function*, *220*(2), 1173–1186.

Gao, W., Gilmore, J.H., Giovanello, K.S., Smith, J.K., Shen, D., Zhu, H., & Lin, W. (2011). Temporal and spatial evolution of brain network topology during the first two years of life. *PLoS ONE*, *6*(9), e25278.

Guy, M.W., Zieber, N., & Richards, J.E. (2016). The cortical development of specialized face processing in infancy. *Child Development*, *87*(5), 1581–1600.

Hammers, A., Allom, R., Koepp, M.J., Free, S.L., Myers, R., Lemieux, L., & Duncan, J.S. (2003). Three-dimensional maximum probability atlas of the human brain, with particular reference to the temporal lobe. *Human Brain Mapping*, *19*(4), 224–247.

Hillebrand, A., Barnes, G.R., Bosboom, J.L., Berendse, H.W., & Stam, C.J. (2012). Frequency-dependent functional connectivity within resting-state networks: An atlas-based MEG beamformer solution. *NeuroImage*, *59*(4), 3909–3921.

Klimesch, W., Sauseng, P., & Hanslmayr, S. (2007). EEG alpha oscillations: The inhibition-timing hypothesis. *Brain Research Reviews*, *53*(1), 63–88.

Mallin, B.M., & Richards, J.E. (2012). Peripheral stimulus localization by infants of moving stimuli on complex backgrounds. *Infancy*, *17*(6), 692–714.

Marshall, P.J., Bar-Haim, Y., & Fox, N.A. (2002). Development of the EEG from 5 months to 4 years of age. *Clinical Neurophysiology*, *113*(8), 1199–1208.

Maslov, S., & Sneppen, K. (2002). Specificity and stability in topology of protein networks. *Science*, *296*(5569), 910–913.

Messaritaki, E., Koelewijn, L., Dima, D.C., Williams, G.M., Perry, G., & Singh, K.D. (2017). Assessment and elimination of the effects of head movement on MEG resting-state measures of oscillatory brain activity. *NeuroImage*, *159*, 302–324.

Miskovic, V., Ma, X., Chou, C.A., Fan, M., Owens, M., Sayama, H., & Gibb, B.E. (2015). Developmental changes in spontaneous electrocortical activity and network organization from early to late childhood. *NeuroImage*, *118*, 237–247.

Oostenveld, R., Fries, P., Maris, E., & Schoffelen, J.M. (2011). FieldTrip: Open source software for advanced analysis of MEG, EEG, and invasive electrophysiological data. *Computational Intelligence and Neuroscience*, *2011*, 156869.

Orekhova, E.V., Stroganova, T.A., & Posikera, I.N. (1999). Theta synchronization during sustained anticipatory attention in infants over the second half of the first year of life. *International Journal of Psychophysiology*, *32*(2), 151–172.

Orekhova, E.V., Stroganova, T.A., & Posikera, I.N. (2001). Alpha activity as an index of cortical inhibition during sustained internally controlled attention in infants. *Clinical Neurophysiology*, *112*(5), 740–749.

Pascual-Marqui, R.D., Lehmann, D., Koukkou, M., Kochi, K., Anderer, P., Saletu, B., & Kinoshita, T. (2011). Assessing interactions in the brain with exact low-resolution electromagnetic tomography. *Philosophical Transactions, Series A, Mathematical, Physical and Engineering Sciences*, *369*(1952), 3768–3784.

Perez-Edgar, K., McDermott, J.N., Korelitz, K., Degnan, K.A., Curby, T.W., Pine, D.S., & Fox, N.A. (2010). Patterns of sustained attention in infancy shape the developmental trajectory of social behavior from toddlerhood through adolescence. *Developmental Psychology*, *46*(6), 1723–1730.

Power, J.D., Fair, D.A., Schlaggar, B.L., & Petersen, S.E. (2010). The development of human functional brain networks. *Neuron*, *67*(5), 735–748.

Reynolds, G.D., & Richards, J.E. (2005). Familiarization, attention, and recognition memory in infancy: An event-related potential and cortical source localization study. *Developmental Psychology*, *41*(4), 598–615.

Reynolds, G.D., & Romano, A.C. (2016). The development of attention systems and working memory in infancy. *Frontiers in Systems Neuroscience*, *10*, 15.

Reynolds, G.D.R., & Richards, J.E. (2008). Infant heart rate: A developmental psychophysiological perspective. In L.A. Schmidt & S.J. Segalowitz (Eds.), *Developmental psychophysiology* (pp. 173–210). Cambridge: Cambridge University Press.

Richards, J.E. (1997). Effects of attention on infants' preference for briefly exposed visual stimuli in the paired-comparison recognition-memory paradigm. *Developmental Psychology*, *33*(1), 22–31.

Richards, J.E. (2003). Attention affects the recognition of briefly presented visual stimuli in infants: An ERP study. *Developmental Science*, *6*(3), 312–328.

Richards, J.E. (2008). Attention in young infants: A developmental psychophysiological perspective. In C.A. Nelson & M. Luciana (Eds.), *Handbook of developmental cognitive neuroscience* (2nd edn.) (pp. 479–497). Cambridge, MA: MIT Press.

Richards, J.E., Boswell, C., Stevens, M., & Vendemia, J.M. (2015). Evaluating methods for constructing average high-density electrode positions. *Brain Topography*, *28*(1), 70–86.

Richards, J.E., Sanchez, C., Phillips-Meek, M., & Xie, W. (2016). A database of age-appropriate average MRI templates. *NeuroImage*, *124*, 1254–1259.

Richards, J.E., & Xie, W. (2015). Brains for all the ages: Structural neurodevelopment in infants and children from a life-span perspective. In J. Benson (Ed.), *Advances in child development and behavior* (Vol. 48, pp. 1–52). Philadelphia, PA: Elsevier.

Rubinov, M., & Sporns, O. (2010). Complex network measures of brain connectivity: Uses and interpretations. *NeuroImage*, *52*(3), 1059–1069.

Shattuck, D.W., Mirza, M., Adisetiyo, V., Hojatkashani, C., Salamon, G., Narr, K.L., & Toga, A.W. (2008). Construction of a 3D probabilistic atlas of human cortical structures. *NeuroImage*, *39*(3), 1064–1080.

Smit, D.J., Boersma, M., Schnack, H.G., Micheloyannis, S., Boomsma, D.I., Hulshoff Pol, H.E., & de Geus, E.J. (2012). The brain matures with stronger functional connectivity and decreased randomness of its network. *PLoS ONE*, *7*(5), e36896.

Sporns, O., & Zwi, J.D. (2004). The small world of the cerebral cortex. *Neuroinformatics*, *2*(2), 145–162.

Stam, C.J., de Haan, W., Daffertshofer, A., Jones, B.F., Manshanden, I., van Walsum, A.M.V., & Scheltens, P. (2009). Graph theoretical analysis of magnetoencephalographic functional connectivity in Alzheimer's disease. *Brain*, *132*, 213–224. https://doi.org/10.1093/brain/awn262

Tzourio-Mazoyer, N., Landeau, B., Papathanassiou, D., Crivello, F., Etard, O., Delcroix, N., & Joliot, M. (2002). Automated anatomical labeling of activations in SPM using a macroscopic anatomical parcellation of the MNI MRI single-subject brain. *NeuroImage*, *15*(1), 273–289.

van den Heuvel, M.P., Kersbergen, K.J., de Reus, M.A., Keunen, K., Kahn, R.S., Groenendaal, F., & Benders, M.J.N.L. (2015). The neonatal connectome during preterm brain development. *Cerebral Cortex*, *25*(9), 3000–3013.

Vertes, P.E., & Bullmore, E.T. (2015). Annual research review: Growth connectomics—the organization and reorganization of brain networks during normal and abnormal development. *Journal of Child Psychology and Psychiatry*, *56*(3), 299–320.

Vinck, M., Oostenveld, R., van Wingerden, M., Battaglia, F., & Pennartz, C.M. (2011). An improved index of phase-synchronization for electrophysiological data in the presence of volume-conduction, noise and sample-size bias. *NeuroImage*, *55*(4), 1548–1565.

Wang, J., Wang, X., Xia, M., Liao, X., Evans, A., & He, Y. (2015). GRETNA: A graph theoretical network analysis toolbox for imaging connectomics. *Frontiers in Human Neuroscience*, *9*, 386.

Watts, D.J., & Strogatz, S.H. (1998). Collective dynamics of 'small-world' networks. *Nature*, *393*(6684), 440–442.

Xie, W., Mallin, B.M., & Richards, J.E. (2018). Development of infant sustained attention and its relation to EEG oscillations: An EEG and cortical source analysis study. *Developmental Science*, *21*(3), e12562.

Xie, W., & Richards, J.E. (2016a). Effects of interstimulus intervals on behavioral, heart rate, and event-related potential indices of infant engagement and sustained attention. *Psychophysiology*, *53*(8), 1128–1142.

Xie, W., & Richards, J.E. (2016b). The relation between infant covert orienting, sustained attention and brain activity. *Brain Topography*, *1*, 1–22.

Ye, A.X., Leung, R.C., Schafer, C.B., Taylor, M.J., & Doesburg, S.M. (2014). Atypical resting synchrony in autism spectrum disorder. *Human Brain Mapping*, *35*(12), 6049–6066.

Yeo, B.T.T., Krienen, F.M., Sepulcre, J., Sabuncu, M.R., Lashkari, D., Hollinshead, M., & Buckner, R.L. (2011). The organization of the human cerebral cortex estimated by intrinsic functional connectivity. *Journal of Neurophysiology*, *106*(3), 1125–1165.

Zhang, Z.Q., Liao, W., Chen, H.F., Mantini, D., Ding, J.R., Xu, Q., & Lu, G.M. (2011). Altered functional–structural coupling of large-scale brain networks in idiopathic generalized epilepsy. *Brain*, *134*, 2912–2928.

SUPPORTING INFORMATION

Additional supporting information may be found online in the Supporting Information section at the end of the article.

How to cite this article: Xie W, Mallin BM, Richards JE. Development of brain functional connectivity and its relation to infant sustained attention in the first year of life. *Dev Sci*. 2018;e12703. https://doi.org/10.1111/desc.12703